Carbohydrate Polymers 79 (2010) 898–907

Contents lists available at ScienceDirect

Carbohydrate Polymers

journal homepage: www.elsevier.com/locate/carbpol

Novel modified starch–xanthan gum hydrogels for controlled drug delivery: Synthesis and characterization

Alireza Shalviri [a], Qiang Liu [b], Mohammad J. Abdekhodaie [a,c], Xiao Yu Wu [a,*]

[a] Department of Pharmaceutical Sciences, Leslie Dan Faculty of Pharmacy, University of Toronto, Toronto, ON, Canada M5S 3M2
[b] Guelph Food Research Center, Agriculture and Agri-food Canada, Guelph, ON, Canada N1G 5C9
[c] Department of Chemical Engineering, Sharif University of Technology, Tehran, Iran

ARTICLE INFO

Article history:
Received 6 July 2009
Received in revised form 9 October 2009
Accepted 9 October 2009
Available online 12 November 2009

Keywords:
Starch–xanthan gum hydrogels
Characterization of cross-links
Equilibrium swelling
Gel mesh size
Solute permeability
Effect of charge and molecular size

ABSTRACT

This work was intended to develop a new cross-linked gelatinized starch–xanthan gum hydrogel system, to characterize the properties of the new material, and to explore its potential applications in controlled drug delivery. Cross-linked starch–xanthan gum polymers were synthesized with varying levels of xanthan gum and sodium trimetaphosphate (STMP). The reaction of starch–xanthan gum polymers with STMP was examined using solid ^{31}P NMR spectroscopy and FTIR. Morphology of the films made from the new polymers was studied by scanning electron microscopy. The swelling properties and the network parameters such as gel mesh size of the films were investigated. The permeation of solutes with various molecular weights and charges across the films was determined. ^{31}P NMR and FTIR spectra showed that both starch and xanthan gum were reacted with STMP. The swelling ratio of the films was higher at higher STMP and xanthan gum levels. The gel mesh size increased with increasing swelling ratio varying from 2.84 to 6.74 nm. Permeability of anionic drugs across the polymeric films was significantly lower than their neutral form due mainly to the electrostatic repulsion between the negatively charged drugs and the polymer. The results suggest that the new cross-linked starch–xanthan gum hydrogels can be potentially used as a film-forming material in controlled release formulations.

1. Introduction

Starch and xanthan gum are polysaccharide-based materials obtained from renewable resources. In addition to broad uses in food products, they have found numerous applications in drug delivery as thickening agents, in coatings, films, hydrogels, microspheres, nanoparticles, and matrix tablets (Bjork & Edman, 1990; Hamdi, Ponchel, & Duchene, 1998, 2001; Jain, Khar, Ahmed, & Diwan, 2008; Krogars et al., 2003; Lenaerts et al., 1998; Mateescu, Ispas-Szabo, & Mulhbacher, 2006; Palviainen et al., 2001; Wierik, Eissens, Bergsma, Arenda-Scholte, & Lerk, 1997). The advantages of these materials also include their cost effectiveness, ease of manufacturing, safety, biocompatibility, and biodegradability.

Starch is one of the most abundant polymers in the nature. It consists of glucose units $(C_6H_{10}O_5)_n$ with n ranging from 300 to 1000. Starch is composed of a mixture of two polymers called amylose and amylopectin. Amylose is a linear polymer with molecular weight of less than 0.5 million Dalton (degree of polymerization of 15×10^2–6×10^3) depending on its botanical source. Amylose macromolecules consist of α-D-glucopyranose units joined by α-1,4 acetal linkages. Amylopectin molecules are much larger and highly branched with molecular weight of 50–100 million Dalton and degree of polymerization of about 3×10^5–3×10^6. The molecules contain α-1,4 linear bounds, and is branched through α-1,6 linkages (Ellis & Ring, 1985; Kerr, 1950).

Xanthan gum is a high molecular weight extracellular heteropolysaccharide with cellulose like backbone. The primary structure of this naturally occurring polymer consists of 1,4 linked β-D-glucose residues, having a trisaccharide side chain of β-D-mannose-β-D-glucuronic acid-α-D-mannose attached to alternate D-glucose units of the main chain (Katzbauer, 1998). The anionic character of this polymer is due to the presence of both glucuronic acid and pyruvic acid groups in the side chain (Kwon et al., 1996). Several groups have reported that relatively small amount of xanthan gum can be used to retard *in vitro* drug release and provide zero-order release kinetics (Baichwal & Staniforth, 1991; Fu Lu, Woodward, & Borodkin, 1991). In addition, it has been shown that xanthan gum tablets can maintain constant drug plasma levels *in vivo* (Talukdar & Plaizier-Vercammen, 1993).

Interaction of starch with hydrocolloids has been well documented in the literature of food science owing to their common coexistence in many food systems and the influence of their interaction on the texture of foods (Abdulmola, Hember, Richardson, & Morris, 1996; Alloncle & Doublier, 1991; Capron, Brigand, & Muller, 1998; Christianson, Honge, Osborne, & Detroy, 1981; Ferrero,

* Corresponding author. Tel.: +1 416 978 5272; fax: +1 416 978 8511.
E-mail address: xywu@phm.utoronto.ca (X.Y. Wu).

0144-8617/$ - see front matter © 2009 Elsevier Ltd. All rights reserved.
doi:10.1016/j.carbpol.2009.10.016

Martino, & Zaritsky, 1994; Mandala & Palogou, 2003; Mandala, Palogou, & Kostaropoulos, 2002). It has been reported that mixing starch with xanthan gum improves the stability and viscosity of the starch gels (Abdulmola et al., 1996; Alloncle & Doublier, 1991; Sudhakar, Singhal, & Kulkar, 1996). Moreover, incorporation of xanthan gum into starch films has been shown to improve some mechanical properties of the starch films such as elongation at break (Veiga-Santos, Oliveira, Cereda, Alves, & Scamparini, 2005). However, at high gum levels phase separation often occurs (Alloncle & Doublier, 1991). To solve this problem, cross-linking was introduced and found to potentially restrict separation of two thermodynamically incompatible biopolymers by either covalently linking the two polymers or by threading one polymer networks through other polymer networks (Rogovina, 1998). Despite the studies in food science, no data on synthesis and characterization of cross-linked modified starch–xanthan gum polymers or their application in controlled drug delivery have been published, to our knowledge. This work is therefore intended to develop a new cross-linked gelatinized starch–xanthan gum hydrogel system, to characterize the molecular structure and functional properties of this new material, and to explore its potential applications in controlled drug delivery.

2. Experimental

2.1. Chemicals and reagents

Corn starch, sodium trimethaphosphate (STMP), pyrogallol red, methylene blue, ibuprofen (sodium salt), caffeine, sodium salicylate, vitamin B12, Fluorescein isothiocyanate-inulin, and Fluorescein isothiocyanate-dextrans with average molecular weight of 4000, 10,000, 21,200, 50,700 were purchased from Sigma-Aldrich Canada (Oakville, ON, Canada). Food grade xanthan gum (Keltrol) was received from Kelco (Rahway, NJ, USA). Sodium sulfate was purchased from Fisher Scientific (Fair Lawn, NJ, USA). All other chemicals were reagent grade and were used as received.

2.2. Synthesis of cross-linked fully gelatinized starch and xanthan gum hydrogels

Ten grams of starch was dispersed in 250 ml of water followed by gradual addition of various amounts of xanthan gum (based on the dry weight of the starch) under vigorous mixing. The mixture was then placed in boiling water bath with vigorous mixing for 1 h. After cooled down to 55 °C, 10 ml of 1 N NaOH was introduced to the mixture. The cross-linking was then initiated by adding different amounts of STMP and 20% sodium sulfate (based on the weight of dry starch). After 5 h the reaction was stopped by neutralizing the pH to 7 with 1 N HCl. The modified starch hydrocolloid polymer was then isolated by centrifugation (4000 rpm x 20 min), washed with water (150 ml × 4) and dried in an air oven at 55 °C. To prepare films, the washed polymer (before it was dried) was dispersed in water to form a homogeneous gel. The gel was then sonicated to reduce air bubbles, poured into Teflon petri dishes, and then dried at room temperature to produce films with average thickness of 0.3–0.4 mm.

2.3. Examination of film morphology

Homogeneity and appearance of the film surface were examined by visual observation. The surface morphology and cross section structure of the films were studied by scanning electron microscopy (SEM) using a Hitachi S3400N variable pressure electron microscope (Tokyo, Japan).

2.4. Confirmation of cross-linking by Fourier transformed infrared (FTIR) spectroscopy

FTIR spectra were recorded on a Perkin-Elmer 1000 series spectrometer (MA, USA). Spectra were taken with a resolution of 4 cm^{-1} and were averaged over 32 scans. Samples were thoroughly grounded with exhaustively dried KBr and pellets were prepared by compression under vacuum.

2.5. Solid state ^{31}P NMR spectroscopy

CP-MAS ^{31}P NMR spectra were obtained using zirconium rotors on a Bruker DSX-200 spectrometer (Rheinstetten, Germany) equipped with 4 mm probe at 200 MHz with a spinning speed of 5 MHz. The modified starch–xanthan gum polymers were grinded using a mortar and pestle and packed into the zirconium rotors. All experiments were performed with contact time of 3 ms, recycle delay of 5 s, and the average of 15,000 scans.

2.6. Study of the swelling behavior of cross-linked starch–xanthan gum polymer

The equilibrium swelling ratio and swelling kinetics of cross-linked starch–xanthan gum polymers with respect to changes in cross-linker level, xanthan gum concentration, and pH were investigated. Circular films with average thickness of 0.3–0.4 mm were placed in 10 ml of buffer solutions of different pH ranging from 2 to12 with ionic strength of 0.15 M or in distilled deionized water (DDIW) at room temperature. Disodium citrate/HCl and phosphate buffer solutions were used for pH 2–4 and pH 5–8, respectively. Diluted NaOH solutions were used for higher pH values. The ionic strength of all the solutions was adjusted to 0.15 M by adding NaCl. After removal from the swelling medium the polymer discs were blotted with filter paper to remove liquid on the sample surface and weighed on a Mettler Toledo AB204-2 analytical balance (Mississauga, Canada). Measurements were taken until equilibrium hydration was reached signaled by the same weight (±0.001 g) in three consecutive measurements. The equilibrium weight swelling ratio (ESR), which represents the ratio of the solvent weight to the polymer weight in the swollen polymer, was calculated using Eq. (1):

$$ESR = \frac{W_s - W_d}{W_d} \quad (1)$$

where W_s represents the swollen weight of the sample at time t and W_d is the dry weight of the sample before swelling.

2.7. Determination of gel mesh size

The average mesh size of modified starch–xanthan gum gels with various degrees of swelling was calculated using Lustig and Peppas theoretical model (Lustig & Peppas, 1988). The model, based on the scaling laws, relates the diffusion coefficient of solutes of known molecular size to structural parameters such as the degree of swelling and the molecular weight between cross-links as described by Eq. (2):

$$\frac{D_i}{D_{i,w}} = \left(1 - \frac{r}{\xi}\right) e^{(-Y/(Q-1))} \quad (2)$$

where D_i and $D_{i,w}$ are the diffusion coefficients of a solute in polymer and in water, respectively; r is the molecular radius of solutes; ξ is the gel mesh size equivalent to the radius of a hollow sphere between neighboring polymer chains; Y is a scale factor for the ratio of the volume displacement per diffusional jump to the free volume contribution per molecule of solvent; and Q is the swelling volume

ratio calculated using the following equation (Hasa & Ilavsky, 1975):

$$Q = 1 + \left(\frac{W_s}{W_d} - 1\right)\frac{\rho_{poly}}{\rho_{solv}} \quad (3)$$

where ρ_{solv} is the density of swelling solvent (e.g. 1 g/cm^3 for water) and ρ_{poly} the density of modified starch–xanthan gum polymer. The density of polymer samples was measured on a device based on the Archimedes principle, using 100% hexane (0.66 g/cm^3) as the test solvent.

To determine the average gel mesh size, the diffusion coefficients of various molecular probes (e.g. FITC-dextran of various molecular weights) across the polymer films were determined. Rearranging Eq. (2) gives Eq. (4):

$$\frac{D_i}{D_{i,w}} = -\frac{r}{\xi}e^{(-Y/(Q-1))} + e^{(-Y/(Q-1))} \quad (4)$$

This equation indicates that plotting $\frac{D_i}{D_{i,w}}$ against r should generate a straight line for a given polymer–solute–solvent system. Linear regression of the plot results in an intercept, $b = e^{(-Y/(Q-1))}$, and a slope, $a = \frac{e^{(-Y/(Q-1))}}{\xi}$ for a general linear equation of $y = -ax + b$. The gel mesh size, ξ, is then calculated using the following relation:

$$\xi = \frac{b}{a} \quad (5)$$

2.8. Permeability studies

The permeability of model drugs in the starch–xanthan gum films with varying STMP and xanthan gum concentrations was measured using side-by-side diffusion cells. Circular films were cut and pre-swollen in buffer solutions of certain pH at 37 °C and their thickness was measured using a micrometer. A pre-swollen sample was then placed between the two cells. After checking for leakage, 3 ml of a drug solution of a known concentration close to saturation concentration was added to the donor cell and 3 ml of buffer solution to the receptor cell. The solution in the receptor cell was transported continuously to a UV cuvette with a peristaltic pump and analyzed using a UV–vis spectrophotometer. From the permeation data, the permeability per unit thickness, P' [cm/s], and the diffusion coefficient of solute, D, were determined using the following equations based on Fick's law of diffusion for the cases when the solute concentration in the donor cell (C_d) is much higher than that in the receptor cell (Kim, 1999):

$$M_t = P'SC_d(t - t_L) \quad (6)$$

$$D = \frac{l^2}{6t_L} \quad (7)$$

$$P' = \frac{DK}{l} \quad (8)$$

In theses expressions, C_d is the initial solute concentration in the donor cell which remains nearly constant during the permeation test; M_t is the accumulative amount of solute in the receptor cell at time t. D, K, l, and t_L are diffusion coefficient, partition coefficient, membrane thickness, and lag time, respectively. S is the effective area of permeation, which is 0.694 cm^2 in this work. Permeability, P', is calculated from the slope of the linear portion of the curve of M_t vs. t at the steady state. To take the thickness of the films into consideration, permeabilities were calculated using Eq. (9).

$$P = P' \times l = DK \ [\text{cm}^2/\text{s}] \quad (9)$$

2.9. Statistical analysis

Data are presented as the mean ± SD for results obtained from three independent experiments unless otherwise indicated. Statistical significance between groups was determined using a one-way ANOVA followed by a post hoc Tukey's Honestly Significant Difference test using SPSS v.16.

3. Results and discussion

3.1. Morphology

The films were macroscopically homogeneous and sufficiently transparent upon visual observation. The SEM images (Fig. 1) show that the film is continuous and homogeneous with few micropores even without use of a plasticizer. The surface of the film is rougher and looser than the cross section with some granular fragments present. The uneven surface may be due to a quite high viscosity of the gel and to the solvent evaporation process.

3.2. Cross-linking of starch–xanthan gum with STMP is confirmed

Fig. 2 presents the FTIR spectra of (A) pure starch, (B) starch reacted with 20% STMP, (C) pure xanthan gum, (D) xanthan gum reacted with 20% STMP, (E) physical mixture of starch and xanthan gum, (F) Physical mixture of starch, xanthan gum, and 20% STMP, and (G) mixture of starch and xanthan gum reacted with 20% STMP. The spectra of starch and xanthan gum both display the typical profile of polysaccharides in the range 920–1100 cm^{-1}

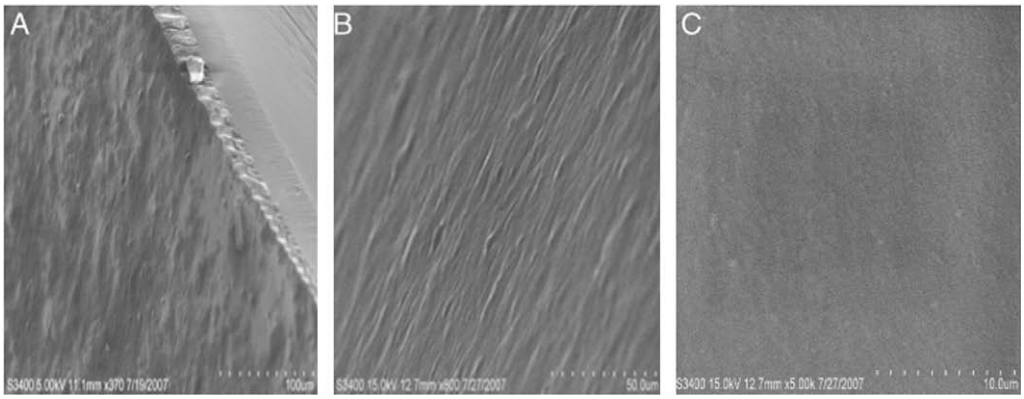

Fig. 1. SEM images of (A) surface (left-bottom corner) and cross section (right-top corner), (B) surface, and (C) cross section of cross-linked starch–xanthan gum film containing 10% xanthan gum and 5% STMP.

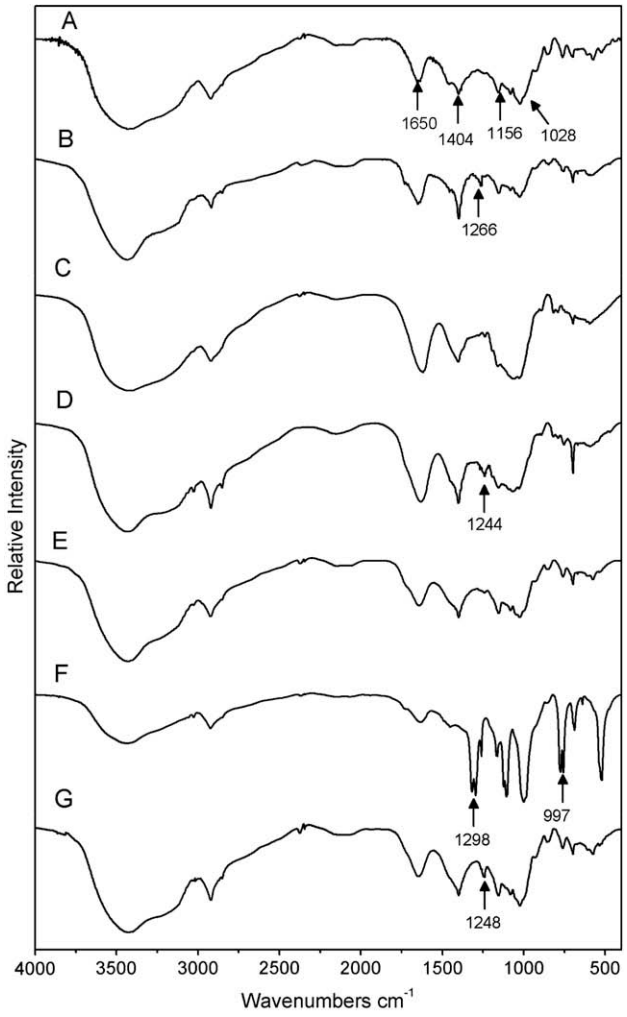

Fig. 2. FTIR spectra of (A) pure starch, (B) starch reacted with 20% STMP, (C) pure xanthan gum, (D) xanthan gum reacted with STMP, (E) physical mixture of starch and xanthan gum, (F) physical mixture of starch, xanthan gum, and STMP, and (G) mixture of starch and xanthan gum reacted with STMP.

(characteristic peaks attributed to CO/CC bond stretching). The peaks at 1028–1084 cm^{-1} are characteristic of the anhydroglucose ring. The peaks at 1404–1410 cm^{-1} are due to OH bending. The peaks at 1645 cm^{-1} are due to the bound water present in the starch and xanthan gum. The band at 2928–2932 cm^{-1} is characteristic of C–H stretching. A broadband due to hydrogen bonded hydroxyl group (O–H) appeared at 3420–3434 cm^{-1} and is attributed to the complex vibrational stretching, associated with free, inter and intra molecular bound hydroxyl groups. The relative intensity of the strong OH stretching band in the native starch, native xanthan gum, and their blend decreased after the reaction with STMP. The physical mixture of starch, xanthan gum and STMP exhibited peaks at 1298 and 997 cm^{-1} due to P═O and P–O bonds, respectively. These peaks disappeared in STMP reacted samples and a new small peak at 1244–1266 cm^{-1} appeared which is the characteristic of P═O bonds in cross-linked polysaccharides. As shown by the reaction scheme in Fig. 3, the reaction of starch or xanthan gum with STMP and the formation of various phosphate products takes place at their –OH groups. Hence the reduction in the –OH stretching band at 3420–3434 cm^{-1} and appearance of P═O at 1244–1266 cm^{-1} suggest that both starch and xanthan gum have reacted with STMP.

Since the modified starch–xanthan gum polymer was neither soluble in water nor was in organic solvents such as DMSO, solid ^{31}P NMR was used to examine the cross-linking of starch and xanthan gum with STMP. Fig. 4A presents the ^{31}P NMR spectra of pure starch (I), starch reacted with STMP (II), pure xanthan gum (III), and xanthan gum reacted with 5% STMP (IV). The spectrum of pure starch does not have any phosphorous peak while the starch reacted with STMP shows two peaks at 0.84 and −12.20 ppm confirming the starch phosphorylation. According to Lack, Dulong, Picton, Cref, and Condamine (2007) and Sang, Prakash, and Seib (2007) the peak at 0.84 ppm represents di-starch phosphate (DSP) and peak at −12.20 ppm corresponds to mono-starch phosphate (MSP) species, respectively. A scheme of the reaction of starch or xanthan gum with STMP and the formation of various phosphate products such as DSP are illustrated in Fig. 3. Apparently only di-polysaccharide phosphates can produce cross-linkages, while mono-polysaccharide phosphates cannot. The starch phosphates could be the combination of mono-, di-, and tri-phosphate species; however, because the peaks obtained from solid NMR are broad and have poor resolution it is not possible to differentiate them.

The xanthan gum reacted with STMP exhibits a very broad peak at −12.26 ppm with a shoulder at about 0.84 ppm and much higher intensity (signal: noise) compared to xanthan gum alone indicating that the polymer is phosphorylated. However, due to the broadness of the peak it is difficult to determine the type of the phosphorous species produced. It is worth mentioning that the xanthan gum reacted with STMP swell but would not dissolve in water, unlike its parent polymer, suggesting the occurrence of cross-linking reaction. Fig. 4B shows the ^{31}P NMR spectra of starch and xanthan gum mixture (I), pure STMP (II), the physical mixture of starch, xanthan gum and STMP (III), and cross-linked starch–xanthan gum (IV), respectively. The peaks at −8.04, 0.41, and 5.77 ppm in the spectrum of the physical mixture correspond to STMP, impurity in xanthan gum, and impurity in STMP, respectively. The reaction of STMP with starch–xanthan gum resulted in disappearance of STMP peak at −8.04 ppm and appearance of two new peaks at −12.5, and 0.77 ppm. The former corresponds to phosphorous species grafting onto a saccharide, and the latter to the cross-linkage formed by one phosphorous group with two saccharides (i.e. phosphate diester).

Fig. 4C shows the NMR spectra of cross-linked starch with 10% xanthan gum and varying amount of STMP (2%, 5%, and 10%). As the amount of cross-linker increases the amount of mono-polysaccharide phosphate species increases. Samples with 2% STMP show a broad peak at 0.40 ppm corresponding to di-polysaccharide phosphate residues and possibly some mono-polysaccharide mono-phosphate (overlapped with the broad peak at 0.40 ppm). At higher STMP levels there are additional peaks at 3.51 and −12.34 ppm attributable to the increase in the amount of mono-polysaccharide mono-phosphate and the appearance of mono-polysaccharide diphosphate species. In summary, the solid NMR study of starch–xanthan gum reacted with STMP confirms the cross-linking of starch, its phosphorylation, and possible cross-linking of xanthan gum. Simultaneous cross-linking of starch and xanthan gum may link the two polymers covalently producing hetero-polymer networks.

3.3. Swelling kinetics and equilibrium swelling ratio

Hydrogel swelling in aqueous media plays a significant role in the biomedical and pharmaceutical applications because it influences: (i) the solute diffusion coefficient through the hydrogels, (ii) the surface properties and surface mobility, and (iii) mechanical properties of the hydrogels. These properties are in turn affected by polymer composition and medium conditions such as pH and ionic strength. The equilibrium swelling and swelling kinetics of the films with varying concentrations of STMP and xanthan gum were

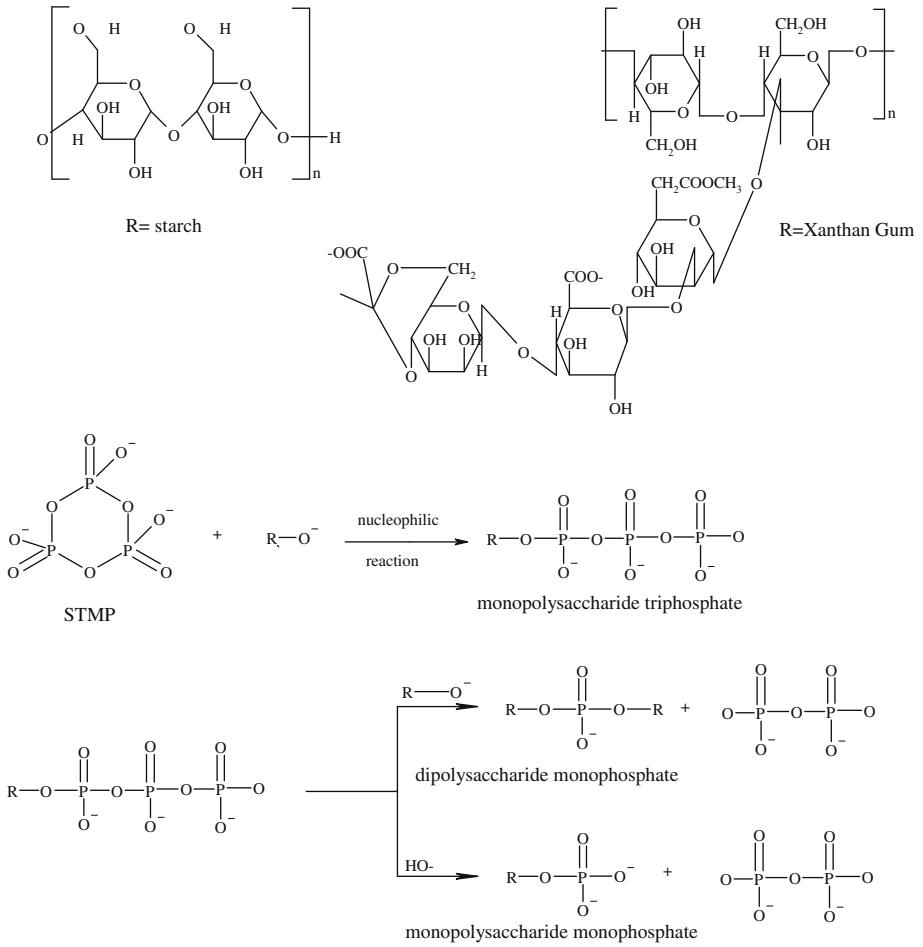

Fig. 3. Schematic representation of cross-linking reaction of starch and xanthan gum with sodium trimethaphosphate (STMP).

studied in DDIW, 0.15 M phosphate buffer of pH 7.4 and buffer solutions of various pH values ranging from 2 to 12. The results are presented in Table 1, Figs. 5 and 6 and described below.

3.3.1. Effect of cross-linker STMP and xanthan gum concentration on the film swelling

As shown in Table 1, the starch–xanthan gum films containing 10% xanthan gum exhibit an unusual swelling behavior with changing STMP concentration. The equilibrium weight swelling ratio, ESR, of the films increases from 2.57 to 9.67 in DDIW and from 1.90 to 6.05 in phosphate buffer solution (PBS) as the STMP level is increased from 0% to 20% (relative to dry starch weight). More dramatic increase in ESR is seen when the STMP content is elevated from 10% to 20%. The positive impact of STMP content on the film swelling is also evidenced by the swelling kinetic studies. Two typical swelling kinetic curves are shown in Fig. 5 for the films containing 5% xanthan gum and two different levels of STMP in 0.15 M phosphate buffer of pH 7.4. Both films swell quickly reaching the plateau in 3 h with the films containing 10% STMP swelling faster and to a higher extent than the films containing 2% STMP.

The influence of xanthan gum content on the equilibrium swelling in DDIW is depicted in Fig. 6A. In general, the swelling ratio increases with increasing xanthan gum concentration due to the hydrophilic nature of the gum, as expected. Interestingly, the films without STMP behave like hydrogels: they swelled rather than dissolving in water. This property may stem from the cold water swellability of gelatinized starch and the formation of helical structure of xanthan gum which is stabilized by the trisaccharide side chains (Chandrasekaran & Radha, 1997; Cui, 2005; Dumitriu, 2005; Iijima, Shinozaki, Hatakeyama, Takahashi, & Hatakeyama, 2007; Stephen, 2006). Nonetheless the films with 5% STMP content swell more than those without STMP.

Normally, an increase in the cross-linking density leads to a lower swelling degree of hydrogels. However, in the case of the STMP cross-linked starch and xanthan gum hydrogels, the reaction with STMP introduces more anionic charges, in addition to cross-linkages. The elevated swelling at higher STMP levels can be ascribed to the ionic nature of the cross-linking agent, the low cross-linking density, and the presence of mono-starch phosphates (see Section 3.2). Possibly, by increasing the amount of STMP beyond a certain value, the cross-linking density increases marginally despite the increase in the content of mono-starch phosphates. As a result, water uptake into the gel becomes faster and greater due to a larger number of negative charges with the addition of the phosphorous species. On the other hand, counter ions remain inside the hydrogel to neutralize the fixed charges on the polymer chains. The high ion concentration can also increase osmotic pressure and thereby high swelling ratio. Furthermore, phosphate groups repel each other due to electrostatic repulsive forces, which cause the expansion of the polymer networks.

This interpretation is supported by the present results of the ^{31}P NMR studies and the findings published by Sang et al. (2007), who proposed that STMP modified starch contained only 0.4% phosphorous content. Moreover, they also showed that the cross-linking reaction results in both di-starch and mono-starch phosphate species. The relative content of these phosphate species appeared to depend on the pH of the reaction medium and more mono-starch phosphate was produced at pH below 10.5. In this work, noticeable

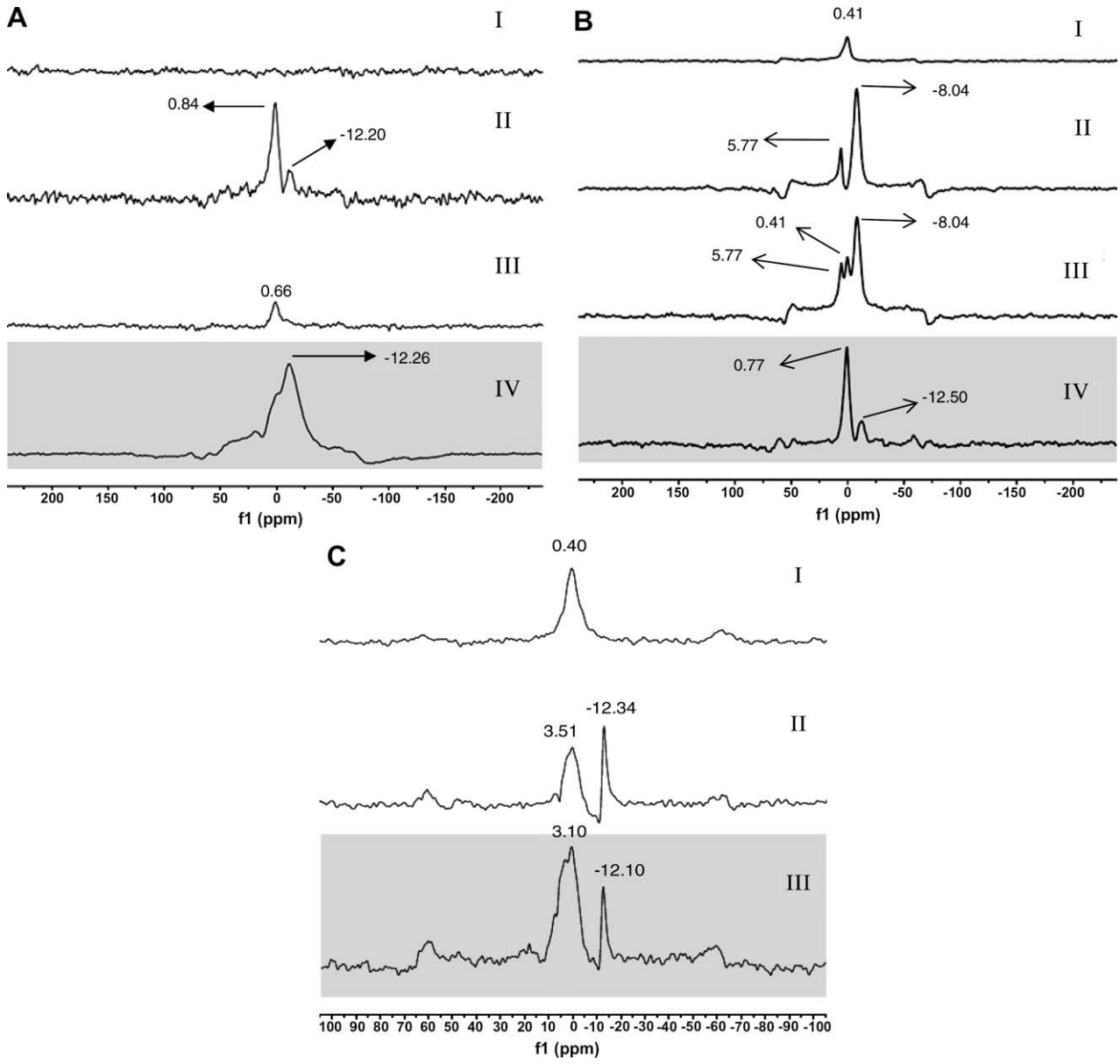

Fig. 4. (A) ^{31}P NMR spectra of (I) pure starch, (II) starch reacted with 5% STMP, (III) pure xanthan gum, (IV) xanthan gum reacted with 5% STMP. (B) ^{31}P NMR spectra of (I) starch–xanthan gum without STMP, (II) STMP, (III) physical mixture of starch, xanthan gum and STMP, (IV) starch and 5% xanthan gum reacted with 5% STMP. (C) ^{31}P NMR spectra of (I) starch and 10% xanthan gum reacted with 2% STMP, (II) starch and 10% xanthan gum reacted with 5% STMP, (III) starch and 10% xanthan gum reacted with 20% STMP.

Table 1
Equilibrium swelling ratio of films with 10% xanthan gum and various cross-linker STMP levels. The data are reported as the mean ± standard deviation of three independent experiments.

STMP level (%)	Equilibrium weight swelling ratio	
	DDIW	PBS (pH = 7.4)
0	*2.57 ± 0.04	*1.90 ± 0.12
2	3.91 ± 0.08	*2.42 ± 0.10
5	3.95 ± 0.20	3.19 ± 0.17
10	*4.71 ± 0.21	3.05 ± 0.07
20	*9.67 ± 0.43	*6.05 ± 0.13

* Statistically significant difference compared to 5% STMP ($P < 0.01$).

peaks at 3.1–3.5 ppm and 12.10 to −12.50 ppm suggest the formation of mono-polysaccharide phosphate bonds in the starch–xanthan gum system, which contributes to higher charge content instead of cross-linking density.

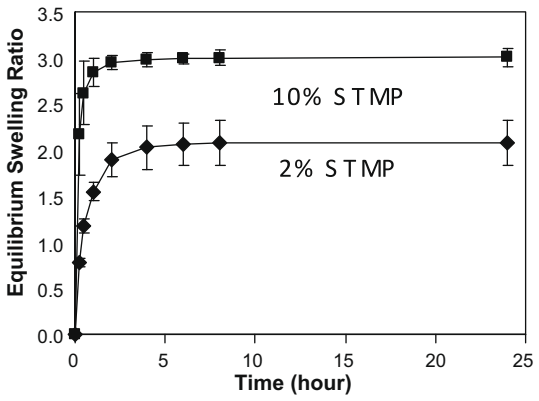

Fig. 5. Swelling kinetics of cross-linked starch–xanthan gum films containing 5% xanthan gum and 2% or 10% STMP in 0.15 M phosphate buffer of pH = 7.4.

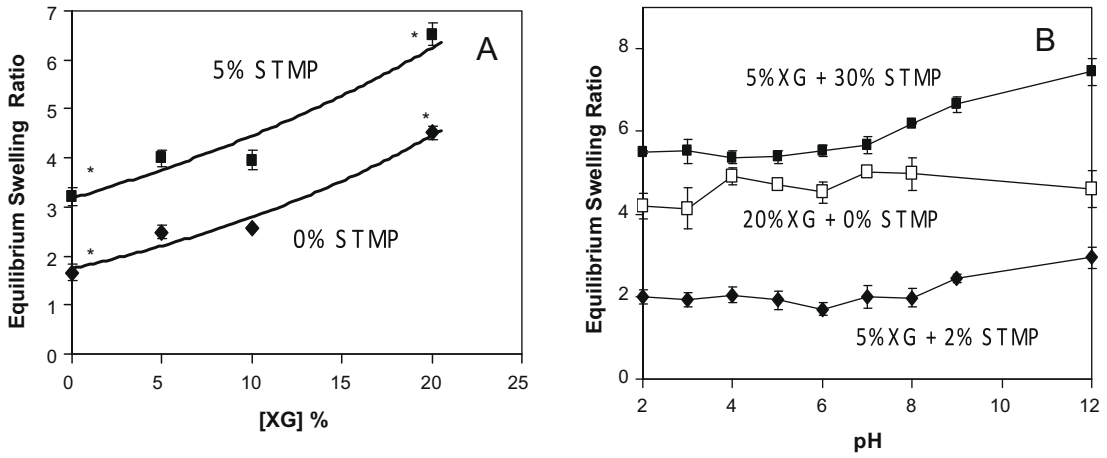

Fig. 6. Equilibrium swelling behavior of modified starch–xanthan gum films of various compositions with respect to change in (A) xanthan gum concentration in DDIW (B) pH with constant ionic strength of 0.15 M. * Statistically significant compared to 5% STMP ($P < 0.05$).

3.3.2. Effect of medium pH and buffer salts on the film swelling

The data in Table 1 and Fig. 6 clearly show that the ESR of the films in DDIW is slightly higher than in PBS of pH 7.4 and ionic strength of 0.15 M. Buffer solutions are different from DDIW in pH and ionic strength. The pH of DDIW is about 6 and contains no electrolyte. To elucidate the role of pH on the ESR of the films, the ESR of various film compositions was determined in buffers of different pH values and a fixed ionic strength of 0.15 M. As illustrated in Fig. 6B, the ESR of the STMP cross-linked films is essentially independent of pH in the buffers with pH values ranging from 2 to 8 and starts to increase at pH 8 and higher. This increase seems more apparent for the films with higher amount of STMP, which might be due to additional ionization of the phosphate species at higher pH values. The structure of the phosphate species is heterogeneous containing mono-, di- and tri-phosphate species. Moreover the location of the phosphorous groups varies with some being covalently bonded directly to the polymer and some apart from the polymers. Therefore, these phosphorous groups may undergo ionization at different pHs. Further investigations are required to delineate this heterogeneity.

The starch–xanthan gum films containing 20% XG without STMP exhibited different pH dependence of ESR from those with STMP. The ESR increases slightly at pH 4, and then decreases from pH 8–12 (Fig. 6B). However, the changes in the ESR of the films without STMP with respect to pH were statistically insignificant.

Both STMP and xanthan gum contribute to the negative charges in the hydrogels giving rise to reduced swelling in PBS as compared to DDIW. The chain expansion in polyelectrolyte gel is reduced by the presence of buffer salts that suppress the Debye length of the electric double layer surrounding the ionic polymer chains, which is reflected by lowered solution viscosity in case of linear polyelectrolytes (Hunkeler, Wu, & Hamielec, 1992; Wu, Hunkeler, Hamielec, Pelton, & Woods, 1991). The effect of small electrolytes on the equilibrium swelling of the gels can be quantitatively described by the following equation for ionic gels (Abdekhodaie & Wu, 2005, 2009; Siegel, 1990):

$$\frac{1}{v}\left[\ln(1-\varphi)+\varphi+\chi\varphi^2\right]+\rho_0\left[\varphi^{\frac{1}{3}}-\frac{\varphi}{2}\right]-\sum(\lambda^{z_i}-1)C_i=0 \qquad (10)$$

where χ, v, and λ are Flory interaction parameter, solvent partial molar volume, and Donnan ratio, respectively; ρ_0 is the density (mol/L) of polymer chains in the network at formation which is twice the density of cross-link points. According to Eq. (10), the polymer volume fraction of the swollen gel, φ, increases; in other words, the swelling ratio decreases with increasing valence of the ionic species, z_i, and the concentration of the mobile ionic species in the solution, C_i. Detailed derivation and calculation examples can be found in the cited publications (Abdekhodaie & Wu, 2005; Siegel, 1990).

3.4. Mesh size of the modified starch–xanthan gum gels

Gel mesh size is an important parameter in characterizing the polymeric networks. It represents the maximum size of diffusing species that can pass through the polymer network, and therefore indicates the screening effect of the network on solute diffusion. Knowing the mesh size of a polymer network enables estimation of the diffusion coefficient of a given drug with known molecular size using Eq. (2). The estimated diffusion coefficient can then be used to predict the drug release rate for a well characterized system.

In this work, diffusion coefficients of FITC-inulin and FITC-dextran with known molecular radii in the modified starch–xanthan gum gels with various compositions and equilibrium volume swelling ratios were calculated using the lag time data obtained from the permeability experiments described earlier. The molecular radii and diffusion coefficients of FITC-inulin and FITC-dextran in water were obtained from literature (Bert, Pearce, Mathieson, & Warner, 1980; Bunim, Smith, & Smith, 1937; Maher, 1989; Wu, 1993). The mesh sizes of the gels were then calculated from the y-intercepts and the slopes of the plots of $\frac{D_i}{D_{i,w}}$ vs. r presented in Fig. 7 using Eq. (5) (Section 2.6). The mesh sizes are listed in Table 2

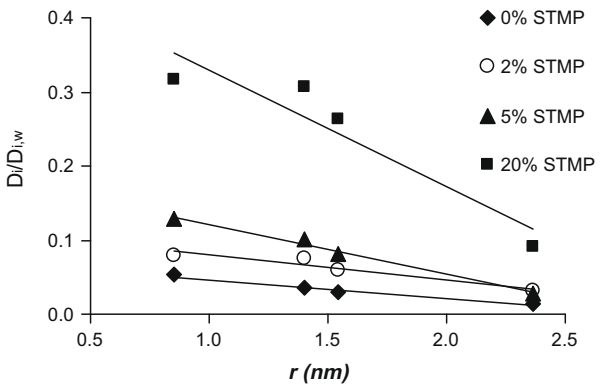

Fig. 7. Relative diffusion coefficients of molecular probes as a function of molecular radius across modified starch–xanthan gum films with various STMP levels.

together with the equilibrium volume swelling ratio, Q, of modified starch–xanthan gum gels containing 10% XG and different cross-linker, STMP, levels. For a fixed XG concentration, the gel mesh size ranged from 2.84 to 6.74 nm and increased with increasing swelling ratio and STMP level. Apparently, for neutral macromolecules, gel swelling degree is a dominant factor for solute diffusion. As the gels swell to a greater degree, the space among polymer chains available for solute to pass through becomes larger, so does the relative diffusion coefficient as shown in Fig. 7.

The y-intercepts of the plots in Fig. 7 were used to calculate Y, a material constant specific to a polymeric system. The natural logarithm of the y-intercepts, extracted from Fig. 7, is plotted against the hydration factors, $(Q-1)^{-1}$, in Fig. 8. From the straight line of the correlation a slope of 7.99 ($r^2 = 0.972$) was obtained which is equivalent to Y.

3.5. Permeability studies

3.5.1. Effect of cross-linker and xanthan gum concentration on permeability

The permeability of vitamin B12 across films with various STMP and xanthan gum concentrations were determined using side-by-side diffusion cells in 0.15 M phosphates buffer of pH 7.4 and the results are summarized in Table 3. As expected, the permeability followed the same trend as the swelling ratio. The permeability increases with increasing STMP content at a fixed XG level of 10%. With 5% STMP, higher XG content resulted in higher permeability.

3.5.2. Effect of molecular size and charge on permeability

The effect of drug molecular size and charge on the permeability was investigated and illustrated in Table 4. In general, permeability increases as the molecular size decreases. However, the permeability of pyrogallol red, a negatively charged compound with $r = 0.54$ nm, was significantly lower than the permeability of vitamin B12, a neutral molecule with $r = 0.85$ nm, and verapamil HCl, a positively charged compound with $r = 0.57$ nm. This abnormal trend may be caused by electrostatic interaction between the drug and the polymer chains. The repulsive forces between the negatively charged drug and the anionic polymer networks may retard drug diffusion in the gel.

To test this hypothesis, the permeabilities of two weakly acidic drugs, ibuprofen and sodium salicylate, in buffer solutions of pH 2 and 7.4 were measured. As shown in Table 5, the permeability of both drugs at pH 2, when they are in protonated form, is 2–3 times higher than that at pH 7.4, when they carry negative charges. Drug transport in hydrogels occurs primarily through water filled regions in the polymer networks. For a given polymer–solvent system, the probability of a solute finding an opening between the polymer chains large enough to permit its passage dictates its diffusivity and is determined by the solute size relative to the mesh size (i.e. r/ξ). For neutral molecules, only the hydration layer of polymer chains in the swollen polymeric network is not accessible to solute diffusion. For charged solute and polymer networks of the same charge, however, the charged surface of polymer chains is also impermeable to the solute due to electrostatic repulsive force, which is equivalent to an increase in the chain thickness or the solute radius by approximately a thickness of Debye length for a constant fiber–fiber distance. In other words, the presence of

Table 2
Equilibrium volume swelling and gel mesh size of starch–xanthan gum gels containing 10% xanthan gum and varying concentrations of cross-linker (STMP). The data are reported as the mean ± standard deviation of three independent experiments.

STMP level (%)	Equilibrium volume swelling ratio (Q)	Mesh size (nm)	Correlation coefficient (r^2)
0	3.89 ± 0.19	2.84	0.968
2	4.68 ± 0.15	3.42	0.918
5	5.84 ± 0.26	4.28	0.972
20	10.20 ± 0.20	6.74	0.977

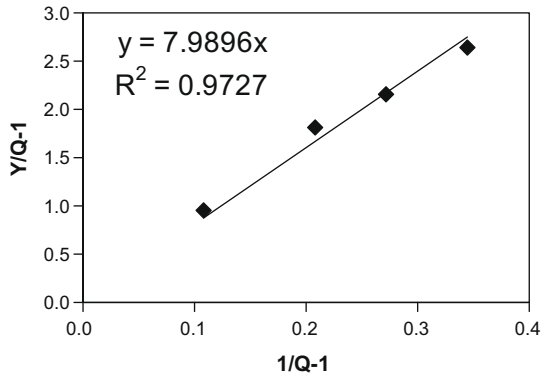

Fig. 8. A plot of $Y/Q - 1$ as a function of the hydration factor $(Q-1)^{-1}$ for starch–xanthan gum hydrogels of various compositions. The slope of the line is equal to the scale factor, Y.

Table 3
Equilibrium swelling ratio of films in 0.15 M phosphate buffer of pH = 7.4 and permeability of vitamin B12 across modified starch–xanthan gum films of various compositions. The data are reported as the mean ± standard deviation of three independent experiments.

Xanthan gum level (%)	STMP level (%)	Equilibrium wt. swelling ratio	Permeability × 10^{-7} cm^2/s
10	0	1.90 ± 0.12	3.10 ± 0.33
10	2	2.42 ± 0.10	3.94 ± 0.33
10	5	3.19 ± 0.17	5.05 ± 0.03
5	5	3.56 ± 0.58	5.20 ± 0.21
20	5	6.50 ± 0.23	6.36 ± 0.56

Table 4
Permeability of macromolecules and drugs of various molecular weights and charges across the starch–xanthan gum gel film containing 10% XG and 5% STMP in 0.15 M phosphate buffer of pH = 7.4. The data are reported as the mean ± standard deviation of three independent experiments.

Drug	MW (g/mol)	Molecular radius (nm)	Charge	Permeability × 10^{-7} (cm^2/s)
FITC-dextran	21200	3.34	Neutral	0.11 ± 0.02
FITC-dextran	10000	2.36	Neutral	0.30 ± 0.02
FITC-dextran	4000	1.54	Neutral	1.53 ± 0.17
Vitamin B12	1355	0.85	Neutral	5.05 ± 0.03
Verapamil HCl	491	0.57	Positive	8.78 ± 0.59
Pyrogallol Red	400	0.54	Negative	2.61 ± 0.41
Methylene Blue	374	0.49	Positive	16.05 ± 1.78
Caffeine	194	0.40	Neutral	33.45 ± 3.10

Table 5
Permeability of two weakly acidic drugs across starch–xanthan gum films containing 10%XG and 5% STMP in pH 2 and 7.4 buffer solutions with ionic strength of 0.15 M. The data are reported as the mean ± standard deviation of three independent experiments.

Drug	pH	MW (g/mol)	Charge	Permeability × 10^{-6} cm^2/s
Ibuprofen sodium salt	2	228.3	Neutral	4.09 ± 0.31
Ibuprofen sodium salt	7.4	228.3	Negative	1.19 ± 0.11
Sodium salicylate	2	160.1	Neutral	3.17 ± 0.45
Sodium salicylate	7.4	160.1	Negative	1.67 ± 0.14

electrostatic repulsive forces between the polymer chain and the drug molecules reduces the free volume available for solute diffusion. The presence of ions in the diffusion layer of the electric double layer also enlarges the hydration layer of polymer chains and the solute, resulting in smaller effective mesh size for solute diffusion and larger hydrodynamic size of the solute. Consequently, the effective ratio of solute radius to mesh size, $(r/\xi)_{eff}$, is increased, so the diffusivity of the solute decreases. Interested reader can refer to literature containing extensive studies (Hwang & Kammermeyer, 1975; Mulder, 1991; Sun, Hsu, & Lai, 2001).

4. Conclusion

Cross-linked starch–xanthan gum hydrogels were successfully synthesized. The synthesis process is straight forward and can be conducted using conventional equipments. The new hydrogel system showed good film forming ability. Both starch and xanthan gum could react with the cross-linker, STMP, thus likely producing hetero-polymer networks. The equilibrium swelling ratio and swelling rate of the starch–xanthan gum hydrogels increased with increasing STMP and XG content especially at concentrations higher than 10%. The unusual dependence of gel swelling on the STMP concentration was ascribed to the formation of mono-polysaccharide phosphate species. The gel mesh size and drug permeability followed the same trend as the gel swelling. The mesh sizes of the hydrogels were determined to be 2.84–6.74 nm at pH 7.4 depending on the gel composition. This mesh size range is large enough for transport of most drugs from small molecules to polypeptide and proteins. The hydrogel exhibited selective permeability depending on drug charges. This selective permeability can be potentially useful for the design of controlled release formulations of ionizable drugs. The results of this work suggest that the new modified starch–xanthan gum hydrogels are a promising material for controlled release formulations for a wide range of drugs and applications.

Acknowledgements

Financial support from Agriculture-Agri-Food Canada and Ben Cohen Fund to A. Shalviri and NSERC operating grant to X.Y. Wu, and technical assistance in the measurement and analysis of IR data from Dr. C. Gordijo and Mr. L. Gordijo are sincerely acknowledged.

References

Abdekhodaie, M., & Wu, X. Y. (2009). Modeling of a glucose sensitive composite membrane for closed-loop insulin delivery. *Journal of Membrane Science, 335*, 21–31.

Abdekhodaie, M., & Wu, X. Y. (2005). Modeling of a glucose-sensitive cationic membrane. *Journal of Membrane Science, 254*, 119–127.

Abdulmola, N. A., Hember, M. W. M., Richardson, R. K., & Morris, E. R. (1996). Effect of xanthan gum on the small-deformation rheology of crosslinked and uncrosslinked waxy maize starch. *Carbohydrate Polymers, 31*, 65–78.

Alloncle, M., & Doublier, J. L. (1991). Viscoelastic properties of maize starch/hydrocolloid pastes and gels. *Food Hydrocolloids, 5*, 455–467.

Baichwal, A. R., & Staniforth, J. N. (1991). Directly compressible sustained release excipient. U.S. Patent Office, Pat. No. 4,994,276.

Bert, J., Pearce, R. H., Mathieson, J. M., & Warner, S. J. (1980). Characterization of collagenous meshworks by volume exclusion of dextrans. *Biochemical Journal, 191*, 761–768.

Bjork, E., & Edman, P. (1990). Characterization of degradable starch microspheres as a nasal delivery for drugs. *International Journal of Pharmaceutics, 62*, 187–192.

Bunim, J. J., Smith, W. W., & Smith, H. W. (1937). The diffusion coefficient of inulin and other substances of interest in renal physiology. *Journal of Biological Chemistry, 118*, 667–677.

Capron, I., Brigand, G., & Muller, G. (1998). Thermal denaturation and renaturation of a fermentation broth of xanthan: Rheological consequences. *International Journal of Biological Macromolecules, 23*, 215–275.

Chandrasekaran, R., & Radha, A. (1997). Molecular modeling of xanthan:galactomannan interactions. *Carbohydrate Polymers, 32*, 201–208.

Christianson, D. D., Honge, J. E., Osborne, D., & Detroy, R. W. (1981). Gelatinisation of wheat starch as modified by xanthan gum, guar gum and cellulose gum. *Cereal Chemistry, 58*, 513–517.

Cui, S. W. (Ed.). (2005). *Food carbohydrates: Chemistry physical properties and applications* (pp. 300). CRC Press.

Dumitriu, S. (Ed.). (2005). *Polysaccharides: Structure diversity and functional versatility* (pp. 470). CRC Press.

Ellis, H. S., & Ring, S. G. (1985). A study of some factors influencing amylose gelation. *Carbohydrate Polymers, 5*, 201–213.

Ferrero, C., Martino, M. N., & Zaritsky, N. E. (1994). Corn starch–xanthan interaction and its effect on the stability during storage of frozen gelatinized suspensions. *Starch/Staerke, 46*, 300–308.

Fu Lu, M., Woodward, L., & Borodkin, S. (1991). Xanthan gum and alginate based controlled release theophylline formulations. *Drug Development and Industrial Pharmacy, 17*, 1987–2004.

Hamdi, G., Ponchel, G., & Duchene, D. (1998). An original method for studying in vitro the enzymatic degradation of cross-linked starch microspheres. *Journal of Controlled Release, 55*, 193–201.

Hamdi, G., Ponchel, G., & Duchene, D. (2001). Formulation of epichlorohydrin cross-linked starch microspheres. *Journal of Microencapsulation, 18*, 373–383.

Hasa, J., & Ilavsky, M. (1975). Deformational, swelling, and potentiometric behavior of ionized poly(methacrylic acid) gels. II. Experimental results. *Journal of Polymer Science. Polymer Physics, 13*, 263–274.

Hunkeler, D., Wu, X. Y., & Hamielec, A. E. (1992). Characterization of polyelectrolytes. In: R. S. Harland & R. K. Prud'homme (Eds.), *Polyelectrolyte gels, properties, preparation, and applications* (pp. 53–79). Washington, DC: American Chemical Society.

Hwang, S. T., & Kammermeyer, K. (1975). *Membranes in separations* (pp. 136–138). New York: Wiley.

Iijima, M., Shinozaki, M., Hatakeyama, T., Takahashi, M., & Hatakeyama, H. (2007). AFM studies on gelation mechanism of xanthan gum hydrogels. *Carbohydrate Polymers, 68*, 701–707.

Jain, A. K., Khar, R. K., Ahmed, F. J., & Diwan, P. V. (2008). Effective insulin delivery using starch nanoparticles as a potential trans-nasal mucoadhesive carrier. *European Journal of Pharmaceutics and Biopharmaceutics, 69*, 426–435.

Katzbauer, B. (1998). Properties and applications of xanthan gum. *Polymer Degradation and Stability, 59*, 81–84.

Kerr, R. W. (1950). *Chemistry and industry of starch*. New York: Academic Press.

Kim, C. (1999). *Controlled release dosage form design*. New York: Informa Healthcare.

Krogars, K., Heinamaki, J., Karjalainen, M., Rantanen, J., Yliruusi, J., & Luukkonen, P. (2003). Development and characterization of aqueous amylose-rich maize starch dispersion for film formation. *European Journal of Pharmaceutics and Biopharmaceutics, 56*, 215–221.

Kwon, G. S., Moon, S. H., Hong, S. D., Lee, H. M., Mheen, T. I., Oh, H. M., et al. (1996). Rheological properties of extracellular polysaccharide, pestan, produced by pestalotiopsis SP. *Biotechnology Letters, 18*, 1465–1470.

Lack, S., Dulong, V., Picton, L., Cref, D., & Condamine, E. (2007). High resolution nuclear magnetic resonance spectroscopy studies of polysaccharides crosslinked by sodium trimetaphosphate: A proposal for the reaction mechanism. *Carbohydrate Research, 342*, 943–953.

Lenaerts, V., Moussa, I., Dumoulin, Y., Mebsout, F., Chouinard, F., Szabo, P., et al. (1998). Cross-linked high amylose starch for controlled release of drugs: Recent advances. *Journal of Controlled Release, 53*, 225–234.

Lustig, S. R., & Peppas, N. A. (1988). Solute diffusion in swollen membranes. IX. Scaling laws for solute diffusion in gels. *Journal of Applied Polymer Science, 36*, 735–747.

Maher, J. F. (1989). *Replacement of renal function by dialysis: A textbook of dialysis*. New York: Springer.

Mandala, I. G., & Palogou, E. D. (2003). Effect of preparation condition and starch xanthan gum concentration on gelation process of potato starch systems. *International Journal of Food Properties, 6*, 311–328.

Mandala, I. G., Palogou, E. D., & Kostaropoulos, A. E. (2002). Influence of preparation and storage conditions on texture of xanthan–starch mixtures. *Journal of Food Engineering, 53*, 27–38.

Mateescu, M. A., Ispas-Szabo, P., & Mulhbacher, J. (2006). Cross-linked starch derivatives for high loaded pharmaceutical formulations. In R. Marchessault & F. Ravenelle (Eds.), *Polysaccharides in drug delivery and pharmaceutical applications* (pp. 121–137). Washington, DC: American Chemical Society Publications.

Mulder, M. (1991). *Basic principles of membranettechnology* (pp. 192–196). Dordrecht: Hluwer.

Palviainen, P., Heinamaki, J., Myllarinen, P., Lahtinen, R., Yliruusi, J., & Forssell, P. (2001). Corn starches as film formers in aqueous-based film coating. *Pharmaceutical Development and Technology, 6*, 353–361.

Rogovina, L. Z. (1998). Approaches to multicomponent systems to biopolymers. *Food Hydrocolloids, 12*, 325–331.

Sang, Y., Prakash, O., & Seib, P. (2007). Characterization of phosphorylated cross-linked resistant starch by ^{31}P nuclear magnetic resonance (^{31}P NMR) spectroscopy. *Carbohydrate Polymers, 67*, 201–212.

Siegel, R. A. (1990). PH-sensitive gels: Swelling equilibria, kinetics, and applications for drug delivery. In J. Kost (Ed.), *Pulsed and self-regulated drug delivery*. Boca Raton: CRC Press.

Stephen, A. M. (Ed.). (2006). *Food polysaccharides and their applications* (pp. 343). CRC Press.

Sudhakar, V., Singhal, R. S., & Kulkar, P. R. (1996). Starch–gum interactions: Nutritional and technological implications. *International Journal of Food Sciences and Nutrition, 47*, 117–129.

Sun, Y. M., Hsu, S. C., & Lai, J. Y. (2001). Transport properties of ionic drugs in the ammonio methacrylate copolymer membrane. *Pharmaceutical Research, 18*, 304–310.

Talukdar, M. M., & Plaizier-Vercammen, J. (1993). Evaluation of xanthan gum as a hydrophilic matrix for controlled-release dosage form preparations. *Drug Development and Industrial Pharmacy, 19*, 1037–1046.

Veiga-Santos, P., Oliveira, L. M., Cereda, M. P., Alves, A. J., & Scamparini, A. R. P. (2005). Mechanical properties, hydrophilicity and water activity of starch–gum films: Effect of additives and deacetylated xanthan gum. *Food Hydrocolloids, 19*, 341–349.

Wierik, G. H. P., Eissens, A. C., Bergsma, J., Arenda-Scholte, A. W., & Lerk, C. F. (1997). A new generation of starch products as excipient in pharmaceutical tablets. II. High surface area retrograded pregelatinized potato starch products in sustained-release tablets. *Journal of Controlled Release, 45*, 25–33.

Wu, C. (1993). Laser light-scattering characterization of the molecular weight distribution of dextran. *Macromolecules, 26*, 3821–3825.

Wu, X. Y., Hunkeler, D., Hamielec, A. E., Pelton, R. H., & Woods, D. R. (1991). Molecular weight characterization of poly(acrylamide-co-sodium acrylate) I. Viscometry. *Journal of Applied Polymer Science, 42*, 2081–2093.